



ELSEVIER

Contents lists available at ScienceDirect

## Journal of Sound and Vibration

journal homepage: [www.elsevier.com/locate/jsvi](http://www.elsevier.com/locate/jsvi)

## Rapid Communication

## A note on safety-relevant vibrations induced by brake squeal

Daniel Hochlenert<sup>a,\*</sup>, Gottfried Spelsberg-Korspeter<sup>b</sup>, Peter Hagedorn<sup>b</sup><sup>a</sup> Institute of Mechanics, Chair of Mechatronics and Machine Dynamics, Technische Universität Berlin, Germany<sup>b</sup> System Reliability and Machine Acoustics, LOEWE-Zentrum AdRIA, Dynamics and Vibrations Group, Technische Universität Darmstadt, Germany

## ARTICLE INFO

## Article history:

Received 4 December 2009

Received in revised form

26 April 2010

Accepted 26 April 2010

Handling Editor: A.V. Metrikine

## ABSTRACT

Brake squeal is mostly considered as a comfort problem only but there are cases in which self-excited vibrations of the brake system not only cause an audible noise but also result in safety-relevant failures of the system. In particular this can occur if lightweight design rims having very low damping are used. Considering the special conditions of lightweight design rims, a minimal model for safety-relevant self-excited vibrations of brake systems is presented. It is shown that most of the knowledge emanated from investigations of the comfort problem can be used to understand and avoid safety-relevant failures of the brake system.

© 2010 Elsevier Ltd. All rights reserved.

## 1. Introduction

Brake squeal is one of the main issues regarding noise, vibration and harshness (NVH) in the development of modern passenger cars. It has become widely accepted by engineers and researchers working in the field that squeal is due to friction-induced, self-excited vibrations of the brake system. The noise-free configuration of the brake system loses its stability and the system then starts oscillating with audible frequencies in a limit cycle, characterized by vibrational amplitudes of several micrometers. A broad overview of brake squeal is given in [1] and a more general review of friction-induced vibrations can be found in [2–4].

There are two common explanations of the self-excitation mechanism. The first one is based on a coefficient of friction decreasing with increasing relative velocity. In this case, the self-excitation can be explained with single-degree-of-freedom models (cf. [3]). However, such a dependence of the friction coefficient does not necessarily occur in a brake system tending to squeal. The second explanation is based on non-conservative forces in the frictional contact. In this case, self-excitation may occur even if the coefficient of friction increases with increasing relative velocity [5]. The corresponding mathematical mechanical models need to have at least two degrees of freedom (see e.g. [6,7]). An overview of minimal models explaining the onset of disk brake squeal is given in [8].

In the context of passenger cars, brake squeal is considered as a comfort problem only, i.e. the noise generated by the brake system does not interfere with its function but is detrimental to the passenger's comfort and lowers the subjective quality of the vehicle. This is quite evident due to the small vibrational amplitudes. However, there are examples in connection with lightweight design rims, in which squeal, i.e. a self-excited vibration of the brake system, may cause safety-relevant failures of the vehicle. A very drastic incident is the failure of spokes of wheels with large diameter, like custom wheels for cars, bicycles and motorcycles due to hub vibrations caused by brake squeal. Similar symptoms of fatigue can be observed on other vehicles with lightweight design rims featuring low damping. To the

\* Corresponding author.

E-mail address: [daniel.hochlenert@tu-berlin.de](mailto:daniel.hochlenert@tu-berlin.de) (D. Hochlenert).

best of the author's knowledge nothing is reported on safety-relevant vibrations excited by squeal in the scientific literature.

The present note is devoted to the mathematical mechanical modeling of brake squeal of vehicles with rims of lightweight design. Considering the special conditions related to lightweight design rims, the minimal model for disk brake squeal presented in [8] is modified and extended. In doing so, a possible explanation of large amplitude vibrations of the hub of lightweight design rims caused by friction-induced vibrations of the brake system is given. Even though the investigation already gives an indication how a safety-relevant failure of the system might be avoided, the present note should be considered as a starting point for further analyses.

## 2. A minimal model for brake squeal of vehicles with lightweight design rims

For the comfort problem of brake squeal a two-degree-of-freedom model was published in [8]. This model consists of a rigid wobbling disk in frictional contact with idealized brake pads and captures the salient features of a disk brake in a rather obvious way. In [9] the rigid wobbling disk was replaced by a rotating Kirchhoff plate. Furthermore, in [10] in- and out-of-plane vibrations of a rotating plate are considered in the context of squeal. All these investigations showed new features related to their specific extension of the model but also confirmed that the basic excitation mechanism is captured by the rigid wobbling disk.

An identical feature of all models is the assumption of a constant speed of rotation of the disk or plate. This is based on the fact that the speed of the vehicle can be considered as constant and the rigid rim yields a constant speed of rotation of the brake disk. In the context of lightweight design rims this assumption should be questioned, since the connection between the hub and the outer rim is rather soft. Moreover the safety-relevant failures and possible fatigue are related to large rotational displacements between the hub and the outer rim. A first minimal model for brake squeal of vehicles with lightweight design rims thus should contain the excitation mechanism of [8] and also allow for the flexible connection between the hub and the outer rim.

The model depicted in Fig. 1 consists of an elastically hinged (stiffness  $k_D$ ) rigid wobbling disk (thickness  $h$ , central moments of inertia  $\Theta, \Phi$ ) which represents the actual flexible brake disk (cf. [8]). The disk is in frictional contact (friction coefficient  $\mu$ ) with idealized brake pads (mass  $m_{P1,2}$ ). Each brake pad is elastically supported by two springs (stiffnesses  $k_2, k_3$ ). The springs with stiffness  $k_3$  are prestressed with the force  $N_0$  guaranteeing contact between the disk and the pads. The system is driven through a visco-elastic coupling (stiffness  $k_H$ , damping  $d_H$ , the shaft in Fig. 1) representing the soft connection between the hub and the outer rim. The (constraint) torque  $M_B$ , originating from the contact force between tire and road, ensures a constant speed of rotation  $\Omega_R$  of the outer rim. This corresponds approximately to a constant speed of vehicle provided that there is no translatory displacement of the hub with respect to the outer rim. By this assumption the dynamics of the tire and the tire–road contact are neglected.

The position of the wobbling disk (body-fixed coordinate system  $\mathbf{d}_i$ ) with respect to the inertial coordinate system  $\mathbf{n}_i$  is described by the three Cardan angles  $q_1, q_2, q_3$ . The brake pads are allowed to move in the  $\mathbf{n}_2$ – $\mathbf{n}_3$  plane only. Their displacements (relative to the equilibrium configuration) are given by  $q_4$  and  $q_5$ , respectively (cf. Fig. 2). The relative twist angle of the visco-elastic coupling, measured from the equilibrium configuration, is denoted by  $q_H$ .

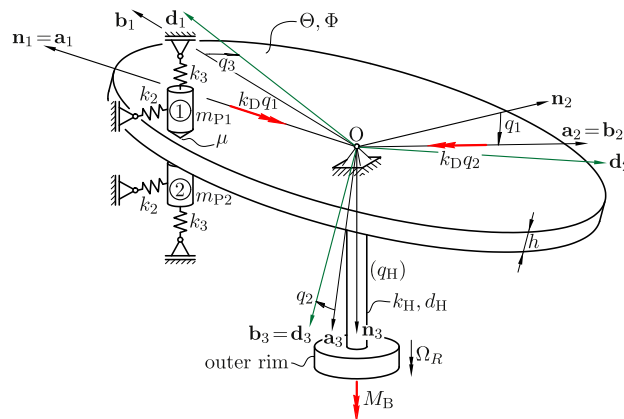


**Fig. 1.** Elastically supported (stiffness  $k_D$ ) wobbling disk in frictional contact with idealized brake pads (mass  $m_{P1,2}$ ) and visco-elastically connected (stiffness  $k_H$ , damping  $d_H$ , relative twist angle  $q_H$ ) to the outer rim rotating at constant speed  $\Omega_R$ .

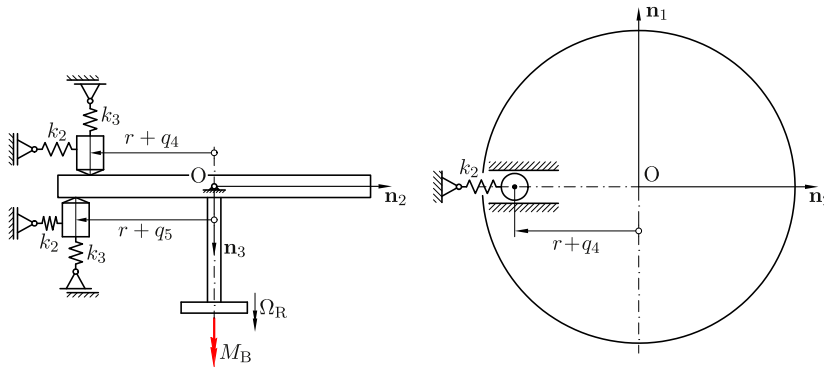


Fig. 2. Side and top of the model shown in Fig. 1 depicting the in-plane displacements the idealized brake pads.

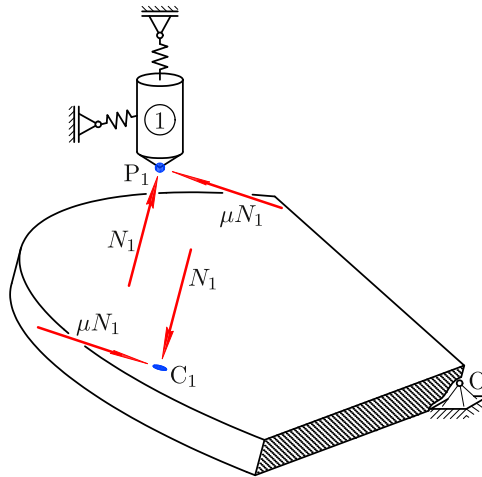


Fig. 3. Labeling of the contact points and forces acting between the disk and pad 1.

2.1. Kinematics

Fig. 3 shows the labeling of the contact points. The position vector from the origin to the tip of the brake pad 1 (point  $P_1$ ) is

$$\mathbf{p}^{O/P_1} = -(r+q_4)\mathbf{n}_2 + \left(x_1 - \frac{h}{2}\right)\mathbf{n}_3 \tag{1}$$

and for the corresponding contact point  $C_1$  on the surface of the disk

$$\mathbf{p}^{O/C_1} = d_{11}\mathbf{d}_1 + d_{12}\mathbf{d}_2 - \frac{h}{2}\mathbf{d}_3 \tag{2}$$

holds, whereas  $x_1$  is the displacement of the spring  $k_3$  and  $d_{11}$ ,  $d_{12}$  are measure numbers to be determined. Since  $P_1$  and  $C_1$  are in contact,

$$\mathbf{p}^{O/P_1} = \mathbf{p}^{O/C_1} \tag{3}$$

yields a system of three linear equations of the unknowns  $x_1$ ,  $d_{11}$ ,  $d_{12}$ . The sequence of rotations described by the Cardan angles  $q_1$ ,  $q_2$ ,  $q_3$  and the intermediate coordinate systems  $\mathbf{a}_i$  and  $\mathbf{b}_i$  lead to the angular velocity

$${}^N\boldsymbol{\omega}^D = \dot{q}_1\mathbf{n}_1 + \dot{q}_2\mathbf{a}_2 + \dot{q}_3\mathbf{b}_3 \tag{4}$$

of the disk with respect to the inertial coordinate system. Therefore, the velocity of  $C_1$  in the inertial coordinate system is given by

$${}^N\mathbf{v}^{C_1} = {}^N\boldsymbol{\omega}^D \times \mathbf{p}^{O/C_1}. \tag{5}$$

The velocity and acceleration of  $P_1$  follows from

$${}^N \mathbf{v}^{P_1} = \frac{N d}{dt} \mathbf{p}^{O/P_1} \quad (6)$$

and

$${}^N \mathbf{a}^{P_1} = \frac{N d^2}{dt^2} \mathbf{p}^{O/P_1}, \quad (7)$$

respectively, i.e. the time derivative of the position vector in the inertial coordinate system. For the calculation of the friction force, the direction of relative velocity of the contact points is needed; it is given by the unit vector

$$\mathbf{r}_1 = \frac{{}^N \mathbf{v}^{C_1} - {}^N \mathbf{v}^{P_1}}{|{}^N \mathbf{v}^{C_1} - {}^N \mathbf{v}^{P_1}|} \quad (8)$$

in the  $\mathbf{d}_1 - \mathbf{d}_2$  plane. Similar relations can be formulated for pad 2. The outer rim rotates at the constant speed of rotation  $\Omega_R$ , such that the constraint

$${}^N \boldsymbol{\omega}^D \cdot \mathbf{n}_3 = \Omega_R + \dot{q}_H \quad (9)$$

holds. The corresponding constraint torque is  $M_B \mathbf{n}_3$ . It is assumed that  $\Omega_R$  is sufficiently large to ensure a non-vanishing relative velocity between the pads and the disk, such that the denominator in (8) is always positive. This assumption holds for squeal typical configurations (see [11,9]). As a consequence, stick-slip phenomena can be excluded in modeling of brake squeal.

## 2.2. Contact forces

Due to the frictional contact, the forces between the pads and the disk act in normal direction and opposed to the relative velocity of the contact points. The normal force acting on pad 1 (on point  $P_1$ ) is

$$\mathbf{N}_1 = -N_1 \mathbf{d}_3. \quad (10)$$

Assuming Coulomb's law of friction and using the direction of the relative velocity (8), the friction force acting on  $P_1$  can be written as

$$\mathbf{R}_1 = \mu N_1 \mathbf{r}_1. \quad (11)$$

The magnitude of the normal force follows from Newton's law formulated for pad 1

$$m_P {}^{P_1} \mathbf{a}^N = \mathbf{N}_1 + \mathbf{R}_1 + (N_0 - k_3 x_1) \mathbf{n}_3 + k_2 q_4 \mathbf{n}_2 \quad (12)$$

projected on the  $\mathbf{n}_3$ - direction. Again, analogous considerations yield the contact forces between pad 2 and the disk.

## 2.3. Equations of motion

The equations of motion of the system follow from the balance of angular momentum for the disk and Newton's law formulated for each brake pad. The latter was already formulated in (12) for pad 1. To obtain a scalar equation, (12) needs to be projected in a direction non-orthogonal to  $\mathbf{n}_2$ . This applies analogously to pad 2. The balance of angular momentum for the disk with respect to the origin reads

$$\frac{N d}{dt} (\mathbf{G}^{D/O} \cdot {}^N \boldsymbol{\omega}^D) = \mathbf{M}^{D/O}, \quad (13)$$

where

$$\mathbf{G}^{D/O} = \Theta \mathbf{d}_1 \otimes \mathbf{d}_1 + \Theta \mathbf{d}_2 \otimes \mathbf{d}_2 + \Phi \mathbf{d}_3 \otimes \mathbf{d}_3 \quad (14)$$

is the central inertia tensor of the disk with respect to the origin and

$$\mathbf{M}^{D/O} = -k_D q_1 \mathbf{n}_1 - k_D q_2 \mathbf{a}_1 - (k_H q_H + d_H \dot{q}_H - M_B) \mathbf{n}_3 - \mathbf{p}^{O/C_1} \times (\mathbf{N}_1 + \mathbf{R}_1) - \mathbf{p}^{O/C_2} \times (\mathbf{N}_2 + \mathbf{R}_2) \quad (15)$$

is the torque acting on the disk with respect to the origin. The constraint (9) can be used to eliminate  $\dot{q}_3$  from the equations of motion yielding the necessary constraint torque  $M_B$ , which can be interpreted as the braking torque of the system. In terms of independent generalized velocities, the resulting system has five degrees of freedom.

The nonlinear equations of motion are very lengthy and can be calculated by the aid of an appropriate multi-body software. The present analysis was performed using the commercial software `Autolev`, which is described in [12]. `Autolev` calculates the equations of motion in analytical form and therefore allows for an analytical linearization as well.

The linearized equations of motion can be written in the form

$$\begin{bmatrix} \mathbf{M}_S & \mathbf{0} \\ \mathbf{0} & \Phi \end{bmatrix} \begin{bmatrix} \ddot{\mathbf{q}}_S \\ \ddot{q}_H \end{bmatrix} + \begin{bmatrix} \mathbf{D}_S + \mathbf{G}_S & \mathbf{0} \\ \mathbf{0} & d_H \end{bmatrix} \begin{bmatrix} \dot{\mathbf{q}}_S \\ \dot{q}_H \end{bmatrix} + \begin{bmatrix} \mathbf{K}_S + \mathbf{N}_S & \mathbf{0} \\ \mathbf{K}_{SH} & k_H \end{bmatrix} \begin{bmatrix} \mathbf{q}_S \\ q_H \end{bmatrix} = \begin{bmatrix} \mathbf{0} \\ 0 \end{bmatrix}, \tag{16}$$

where

$$\mathbf{q}_S = [q_1 \ q_2 \ q_4 \ q_5]^T \tag{17}$$

contains all generalized coordinates of the system except the relative twist angle  $q_H$  of the visco-elastic coupling. The sub-matrices in (16) read

$$\mathbf{M}_S = \begin{bmatrix} \Theta + (m_{p1} + m_{p2})r^2 & 0 & 0 & 0 \\ -\frac{1}{2}\mu(m_{p1} + m_{p2})hr & \Theta & 0 & 0 \\ 0 & 0 & m_{p1} & 0 \\ 0 & 0 & 0 & m_{p2} \end{bmatrix},$$

$$\mathbf{D}_S + \mathbf{G}_S = \begin{bmatrix} \frac{\mu N_0 h^2}{2\Omega_R r} & \Omega_R \Phi & -\frac{\mu N_0 h}{2\Omega_R r} & \frac{\mu N_0 h}{2\Omega_R r} \\ -\Omega_R \Phi & 0 & 0 & 0 \\ -\frac{\mu N_0 h}{2\Omega_R r} & 0 & \frac{\mu N_0}{\Omega_R r} & 0 \\ \frac{\mu N_0 h}{2\Omega_R r} & 0 & 0 & \frac{\mu N_0}{\Omega_R r} \end{bmatrix},$$

$$\mathbf{K}_S + \mathbf{N}_S = \begin{bmatrix} k_D + hN_0 + 2k_3r^2 & \frac{\mu N_0 h^2}{2r} & -N_0 & N_0 \\ -\mu r(2N_0 + hk_3) & k_D + (1 + \mu^2)hN_0 & 0 & 0 \\ -N_0 & \frac{h\mu N_0}{2r} & k_2 & 0 \\ N_0 & \frac{h\mu N_0}{2r} & 0 & k_2 \end{bmatrix},$$

$$\mathbf{K}_{SH} = [0 \ 0 \ -\mu N_0 \ -\mu N_0].$$

It should be noted that the linearized system is coupled in a one-sided fashion, i.e. the last row of (16) is coupled with the rest of the system via  $\mathbf{K}_{SH}$ , whereas  $q_H$  has no influence on the rest of the system. This will be discussed in the following stability analysis.

#### 2.4. Stability analysis

Due to the one-sided coupling, the stability of the system (16), i.e. the stability of the trivial solution of the nonlinear system, is determined by the subsystem

$$\mathbf{M}_S \ddot{\mathbf{q}}_S + (\mathbf{D}_S + \mathbf{G}_S) \dot{\mathbf{q}}_S + (\mathbf{K}_S + \mathbf{N}_S) \mathbf{q}_S = \mathbf{0}, \tag{18}$$

which has the same structure as the minimal model proposed in [8]. In fact, for  $q_4 \equiv q_5 \equiv 0$  and  $m_{p1,2} = 0$  the system (18) is identical to the one of [8]. Therefore, a detailed stability analysis of (18) with respect to the system's parameters is not repeated here. However, it should be emphasized that (18) has a pair of eigenvalues with positive real part for realistic parameters and thus shows self-excited vibrations, which are interpreted as the onset of squeal. In this case, the non-decaying part of the solution of (18) can be written as

$$\mathbf{q}_S(t) = \hat{\mathbf{q}}_S e^{\delta_S t} \sin(\omega_S t + \gamma_S), \tag{19}$$

where  $\lambda_S = \delta_S \pm i\omega_S$  is the complex conjugated pair of eigenvalues having a positive real part ( $\delta_S > 0$ ) and  $\hat{\mathbf{q}}_S, \gamma_S$  are constants to be calculated from the initial conditions. In the case of brake squeal,  $\omega_S$  is approximately the frequency of squeal and the exponentially growing amplitudes are limited by nonlinear effects resulting in a limit cycle with an amplitude of several micrometers [13].

The focus of the present analysis is on the influence of the self-excited vibrations on  $q_H$ , that is the twist of the hub-rim system. As mentioned in the Introduction, safety-relevant failures caused by squeal phenomena may arise in the context of lightweight design rims. These failures are directly related to the twist of the hub in the outer rim. Considering the last row of (16) for  $\mathbf{q}_S(t)$  given in (19) yields

$$\Phi \ddot{q}_H + d_H \dot{q}_H + k_H q_H = \hat{f} e^{\delta_S t} \sin(\omega_S t + \alpha_S), \tag{20}$$

with  $\hat{f} = -\mathbf{K}_{SH}\hat{\mathbf{q}}_S$ . A particular solution of (20) is

$$q_H(t) = C_H e^{\delta_S t} \sin(\omega_S t + \alpha_S - \gamma_H), \quad (21)$$

where the constants  $C_H$ ,  $\gamma_H$  are given by

$$C_H = |H|, \quad \gamma_H = \arg(H), \quad H = \frac{\hat{f}/\Phi}{2(i\omega_S + \delta_S)(\delta_S + \delta_H) - \delta_S^2 + (\omega_H^2 - \omega_S^2)} \quad (22)$$

and  $\omega_H^2 = k_H/\Phi$  and  $2\delta_H = d_H/\Phi$  are the eigenfrequency and damping ratio of the hub–rim system. Typically the hub–rim system has a very low damping such that, if the frequency of squeal is close to eigenfrequency of the hub–rim system ( $\omega_S \approx \omega_H$ ), the constant  $C_H$  is very large. Therefore, due to resonance effects, the magnitude of the twist angle  $q_H$  will become very large even if the limit cycle corresponding to  $\hat{\mathbf{q}}_S$  has an amplitude in the micrometer range only. The actual amplitudes of the resulting limit cycle oscillations are determined by nonlinearities of the system. The nonlinear equations of motion are of course coupled in a two-sided fashion but considering the response of the linearized system as a generating solution of the nonlinear system, the amplitude of the twist angle  $q_H$  will be much larger than the magnitude of vibrations of the brake system. To the author's knowledge, safety-relevant failures indeed arose in systems where the resonance condition  $\omega_S \approx \omega_H$  was met and the issue was solved by a modification of the rim, changing  $\omega_H$  in order to keep the oscillations of the hub–rim system as small as possible. Further details on the practical problem are omitted due to confidentiality.

### 3. Conclusions and outlook

Based on a minimal model it was shown how safety-relevant vibrations can be induced by brake squeal. Due to resonance effects, the amplitudes of the safety-relevant vibrations are orders of magnitudes larger than the amplitudes of noise-emitting vibrations of the brake system. Such resonance effects are likely to occur in the context of lightweight design rims featuring a soft and lowly damped connection between the hub and the outer rim. Since the present minimal model is based on the generally accepted excitation mechanism of brake squeal, most of the knowledge emanated from investigations of the comfort problem can be directly applied. Furthermore, the one-sided fashion of the coupling between the brake and the hub–rim system is maintained as long as additional parts are connected to boundaries of present minimal model.

The analysis showed that avoiding the resonance effect is a remedy for safety-relevant problems. However, the minimal model highlights the excitation mechanism in a synthetic fashion only and should be considered as a starting point for further analyses or as a benchmark problem for commonly used commercial multi-body or finite element codes.

### References

- [1] N.M. Kinkaid, O.M. O'Reilly, P. Papadopoulos, Automotive disc brake squeal, *Journal of Sound and Vibration* 267 (2003) 105–166.
- [2] R. Ibrahim, Friction-induced vibration, chatter, squeal and chaos, part I: mechanics of contact and friction, *Applied Mechanics Reviews* 47 (7) (1994) 209–226.
- [3] R. Ibrahim, Friction-induced vibration, chatter, squeal and chaos, part II: dynamic and modeling, *Applied Mechanics Reviews* 47 (7) (1994) 227–253.
- [4] G. Sheng, *Friction-Induced Vibrations and Sound: Principles and Applications*, CRC Press, Boca Raton, 2008.
- [5] E. Brommundt, Ein Reibschwinger mit Selbsterregung ohne fallende Reibkennlinie, *Zeitschrift für Angewandte Mathematik und Mechanik* 75 (11) (1995) 811–820.
- [6] K. Popp, M. Rudolph, M. Kröger, M. Lindner, Mechanisms to generate and avoid friction induced vibrations, *VDI-Bericht* 1736 (2002) 1–15.
- [7] N. Hoffmann, M. Fischer, R. Allgaier, L. Gaul, A minimal model for studying properties of the mode-coupling type instability in friction induced oscillations, *Mechanics Research Communications* 29 (2002) 197–205.
- [8] U. von Wagner, D. Hochlenert, P. Hagedorn, Minimal models for disk brake squeal, *Journal of Sound and Vibration* 302 (2007) 527–539.
- [9] D. Hochlenert, G. Spelsberg-Korspeter, P. Hagedorn, Friction induced vibrations in moving continua and their application to brake squeal, *ASME Journal of Applied Mechanics* 74 (2007) 542–549.
- [10] G. Spelsberg-Korspeter, D. Hochlenert, O.N. Kirillov, P. Hagedorn, In- and out-of-plane vibrations of a rotating plate with frictional contact: investigations on squeal phenomena, *ASME Journal of Applied Mechanics* 76 (4) (2009) 041006–1–15.
- [11] H. Hetzler, W. Seemann, Friction modes in low frequency disc-brake noise—experimental results and effects on modelling, *Proceedings in Applied Mathematics and Mechanics* 6 (2006) 307–308.
- [12] T. Kane, D. Levinson, *Dynamics: Theory and Applications*, McGraw-Hill, New York, 1985.
- [13] D. Hochlenert, Nonlinear stability analysis of a disk brake model, *Nonlinear Dynamics* 58 (1) (2009) 63–73.